Slow and stopped light in metamaterials: the trapped rainbow

Kosmas L. Tsakmakidis and Ortwin Hess*
Advanced Technology Institute and Department of Physics, Faculty of Engineering and Physical Sciences, University of Surrey, Guildford, GU2 7XH, United Kingdom

ABSTRACT

We show how guided electromagnetic waves propagating along an adiabatically tapered negative-refractive-index metamaterial heterostructure can be brought to a complete halt. It is analytically shown that, in principle, this method simultaneously allows for broad bandwidth operation (since it does not rely on group index resonances), large delay-bandwidth products (since a wave packet can be completely stopped and buffered indefinitely) and high, almost 100%, in/out-coupling efficiencies. By nature, the presented scheme invokes solid-state materials and, as such, is not subject to low-temperature or atomic coherence limitations. A wave analysis, which demonstrates the halting of a monochromatic field component travelling along the heterostructure, is followed by a pertinent ray analysis, which unmistakably illustrates the trapping of the associated light-ray and the formation of a double light-ray cone ('optical clepsydra') at the point where the ray is trapped. This method for trapping photons conceivably opens the way to a multitude of hybrid optoelectronic devices to be used in 'quantum information' processing, communication networks and signal processors and may herald a new realm of combined metamaterials and slow light research.

Keywords: Slow light, metamaterials, negative refractive index, waveguides, adiabatic variation

1. INTRODUCTION

A far-reaching development in modern nanophotonics and nanoengineering has been the conception and practical implementation of materials exhibiting simultaneously negative electric permittivity and magnetic permeability, known also as left-handed metamaterials (LH-MMs). Their conceivable strong economic and social impact, owing to their potential applicability in diverse realms of science, such as telecommunications, radars and defence, nanolithography with light, microelectronics, medical imaging, and so on, has lately prompted an overwhelming excitement within the scientific community [1]-[3].

The history of MMs appears to be dating back to the pioneering work of Kock [4] in the late 40's; while working at Bell Labs with Sergei Schelkunoff, renowned for his "field equivalence principles" and for his work on antennas theory, Kock published a series of works wherein he proposed numerous ideas for constructing lightweight and small-volume "artificial dielectrics", used as microwave lenses in antenna systems. Amongst others, he studied the response to an incident quasi-static electromagnetic radiation of isolated or regularly-arrayed metallic particles of various shapes, such as spheres, discs, ellipsoids and prolate or oblate spheroids. He concluded that such structures effectively behave as a dielectric medium, whose permittivity ε and permeability μ can be purposely tuned (but not independently of each other) to an arbitrarily large or small, even negative, value by properly arranging the particles in three dimensions, i.e. the optical properties of the medium depended solely on the particles' geometrical set up, rather than on their own intrinsic behaviour. Kock also showed that a specially-designed structure, which lately has come to be known as "split-ring resonator" (SRR), can be used to independently increase the permeability μ, such that one can reduce or altogether eliminate the diamagnetic nature of the aforementioned composite structures. His work rose considerable interest within the engineering community of the time, with a number of works extending or elaborating on his ideas. Since then, it has been the subject of detailed coverage in standard engineering textbooks [5].

* O.Hess@surrey.ac.uk; phone +44 (0) 1483 682745; fax +44 (0) 1483 686081.

Metamaterials III, edited by Nigel P. Johnson, Ekmel Özbay, Nikolay I. Zheludev, Richard W. Ziolkowski
Proc. of SPIE Vol. 6987, 698702, (2008) · 0277-786X/08/$18 · doi: 10.1117/12.786348

More than a decade later, Rotman [6] also considered the quasi-static response of an array of thin conducting wires, and he showed that such a structure closely resembles, on the macroscopic level, a plasma medium. In particular, he proved that the electric permittivity ε of this artificial dielectric medium varies with frequency following a Drude-type law. Consequently, below a certain "cutoff" frequency no incident electromagnetic radiation could penetrate it. Critically, however, neither Kock nor Rotman or, indeed, any of the early contributors investigated the properties of media exhibiting concurrently negative ε and μ. Partly, that was because the main motivation behind similar works at that time was to design plasma media at RF or microwave frequencies that would closely simulate the ionosphere, prompted by NASA's desire to secure the safe re-entrance of space-capsules into the earth's atmosphere.

Veselago [7] was evidently the first to systematically consider, in the late 60's, the possibility and some properties of "double-negative materials" (DNGMs). In particular, he showed that a negative electric permittivity ε and magnetic permeability μ would imply a reversal of almost all known electromagnetic phenomena, including the angle of refraction inside a DNGM, the Doppler effect, the sign of the refractive index n (e.g., $n = -1$) and the right-handedness of the **E**, **H** and **k** vector-triad, from where the designation of such materials as "left-handed" origins. In spite of his noteworthy findings, and apparently unaware of Kock's and other workers' research in the same field, Veselago did not go on to materialise his theoretical conclusions. Even so, his work did not go unnoticed and he was invited several times to highlight his research at major international scientific conferences [8].

At present, the realm of "artificial dielectrics" or "metamaterials" (from the Greek word "meta", which here means "beyond") enjoys a breadth of scientific activity and exploration, having established a sound and coherent mathematical formalism, the predictions of which have been verified by numerous experimental and numerical-simulation works. This revived interest followed from a series of works by Pendry, wherein he proposed practical means for realizing LH-MMs experimentally [9]. Moreover, building on Veselago's work, Pendry argued that a slab constructed by the same materials could, ideally, act as a "perfect lens", overcoming the well-known diffraction limitations. After these insights, the physical construction of a composite LH structure has been demonstrated by Shelby et al. [10], and the possibility of achieving subwavelength resolution of an object with the same structure has been demonstrated with further experiments [11]. By now there is compelling evidence that, via building on familiar transmission-line concepts borrowed from microwave analysis, these materials can be designed to exhibit broadband negative-index behaviour and relative robustness to losses, all through the microwave up to the ultraviolet domain [12, 13].

During the same period and in parallel with the above advances a different, also exciting, realm of contemporary research has also been witnessing impressive progress. The goal in this field was to produce "slow" or completely "stopped" light, i.e. electromagnetic waves in the optical and telecommunication regimes with extremely small group velocities compared to the speed of light in vacuum ($v_g << c$) [14]. Such an ability to controllably decelerate, stop, store and regenerate / release optical pulses in a low-loss regime, will conceivably have important potential applications, ranging from quantum memories for photons and storage of light, to the realisation of optical buffers for photonic communication networks.

Until now, a variety of methods have been proposed as a means of producing "slow" or "stopped" light, including electromagnetically induced transparency (EIT) [15], quantum-dot semiconductor optical amplifiers (QD-SOAs) [16], photonic crystals (PCs) [17], coherent population oscillations (CPOs) [18], stimulated Brillouin scattering (SBS) [19] and surface plasmon polaritons (SPPs) in metallodielectric waveguides [20, 21]. However, so far, most of these methods bear inherent limitations that may hinder their practical deployment. For instance, EIT uses ultracold atomic gases (e.g. a cloud of sodium atoms at a temperature of 0.9 μK) and not solid state materials, QD-SOAs usually allow for only modest delays but for potentially ultra-broadband light pulses, CPOs and SBS are very narrowband (typically, several MHz) owing to the narrow transparency window of the former and the narrow Brillouin gain bandwidth of the latter, SPPs are very sensitive to surface roughness and are relatively difficult to excite, while PCs may be highly multimodal; this, combined with the strong impedance mismatch in the "slow-light regime" makes launching the incoming light energy to a single, slow mode alone overly difficult.

In what follows we show that efficient slow and stopped light can be realized inside axially varying, adiabatically tapered, NRI waveguide heterostructures. This method for producing "slow-light" turns out to be remarkably simple and bears a number of serious advantages compared to previously proposed ways of decelerating optical signals. The

heterostructures investigated here can be designed for monomode operation in the desired frequency range, while the control of the group velocity can be achieved by appropriate tuning of the microphotonic structure, either through laser thermo-optic illumination to locally modify the refractive index, or via optically-induced attractive/repulsive forces exerted on the heterostructures to manipulate the thickness of its core. We prove that the same is also true for the light in- and outcoupling, which can be satisfactorily adjusted by adiabatically tapering the thickness of waveguide core. Finally, it is shown that the present mechanism for decelerating and trapping light does not rely on group index resonances, and therefore broadband slow light can be obtained provided that the negative material parameters are designed to exist over relatively large bandwidths, with low losses, at optical frequencies, as highlighted above [12, 13].

2. SLOW LIGHT IN ADIABATICALLY TAPERED NEGATIVE-INDEX HETEROSTRUCTURES

In this section we investigate the propagation of light along a waveguide with a slowly, axially varying negative refractive index (NRI) core. In particular, we analytically prove that at a pre-arranged core thickness, the guided lightwave is altogether halted. We derive an expression for the effective guide thickness, and connect it to time-averaged power flow propagating in the increasing (forward) $+z$ direction. Finally, our analysis reveals that NRI heterostructures can facilitate very efficient butt-coupling from a conventional, right handed, dielectric waveguide.

2.1 Adiabatically tapered NRI waveguide

For the applicability of the adiabatic approximation one needs to ensure that the variation of core half-thickness α with propagation distance z (see Fig. 1) is properly slow. Starting from Maxwell's equations and by deploying coupled-mode theory, we can formally show [22, Chs. 19 & 28] that the requirement for slow core thickness variation is fulfilled when the length of each tapered waveguide segment is large compared with the largest distance over which the guided fields can change appreciably owing to phase differences between the supported local modes. This leads to the following 'axial variation criterion':

$$\frac{d\alpha}{dz} << \frac{\alpha(\beta_2 - \beta_3)}{2\pi}, \tag{1}$$

where β_2 and β_3 are the scalar propagation constants of the second- (m = 1) and third-order (m = 2) backward waveguide modes TM^{b}_{m+1} of the NRI waveguide [23]. This criterion can also take the form:

$$\frac{d\alpha}{dz} << \frac{(\alpha k_0)\Delta n_{eff}^{2,3}}{2\pi}. \tag{2}$$

The electromagnetic fields $\mathbf{G} = \mathbf{E}$ or $\mathbf{H}$ at a distance $z = z_t$ inside an axially varying left-handed heterostructure (LHH), which satisfies the above criterion, are given by:

$$\mathbf{G}(x, y, z_t, t) = F(z_t)\mathbf{g}(x, y, \beta(z_t))\exp\left[i \sum_{z=0}^{z=z_t} \beta(z)\Delta z - i\omega t \right]. \tag{3}$$

Here the parameter F, which is the positive constant used in the solution ansatz to the wave equation (see Eq. (14)), is chosen in such a way that $\partial P_{\mathrm{tot}}^{\mathrm{con}}/\partial z = 0$, where $P_{\mathrm{tot}}^{\mathrm{con}} = \sum_{i=1}^{3} | P_i^{+z} |$ is the conserved total time-averaged power flow in the LHH [23, 24, 28] and P_i^{+z} the time-averaged power flow in the i-layer (i = 1, 2, 3), propagating in the increasing $+z$ direction. In order to enforce the conservation of $P_{\mathrm{tot}}^{\mathrm{con}}$ in the analytic computations, we normalize the fields in such a

way that, at each tapered waveguide segment, they carry a total (conserved) time-averaged power flow equal to $P_{\text{tot}}^{\text{con}}$. To this end, we start by calculating $P_i^{+z} = 1/2 \int_{A_i} \text{Re}(\mathbf{E} \times \mathbf{H}^*)_z \, dA$ in each waveguide layer and, after some algebraic manipulations [23, 24], we arrive at:

$$P_{\text{tot}}^{\text{con}} = \frac{F^2}{4\omega\varepsilon_0} \frac{\alpha\beta}{|\varepsilon_{r1}|} \frac{W_3^2 + \sigma_\varepsilon^2 U^2}{\sigma_\varepsilon^2 U^2} \left(2 + \frac{\rho_\varepsilon}{W_2} \frac{U^2 - W_2^2}{W_2^2 + \rho_\varepsilon^2 U^2} + \frac{\sigma_\varepsilon}{W_3} \frac{U^2 - W_3^2}{W_3^2 + \sigma_\varepsilon^2 U^2} \right), \tag{4}$$

where $\sigma_\varepsilon = \varepsilon_{r3} / |\varepsilon_{r1}|$, $\rho_\varepsilon = \rho_{r3} / |\rho_{r1}|$, W_2 and W_3 are the reduced decay constants of the second and third layer, respectively, and U is the reduced transverse constant.

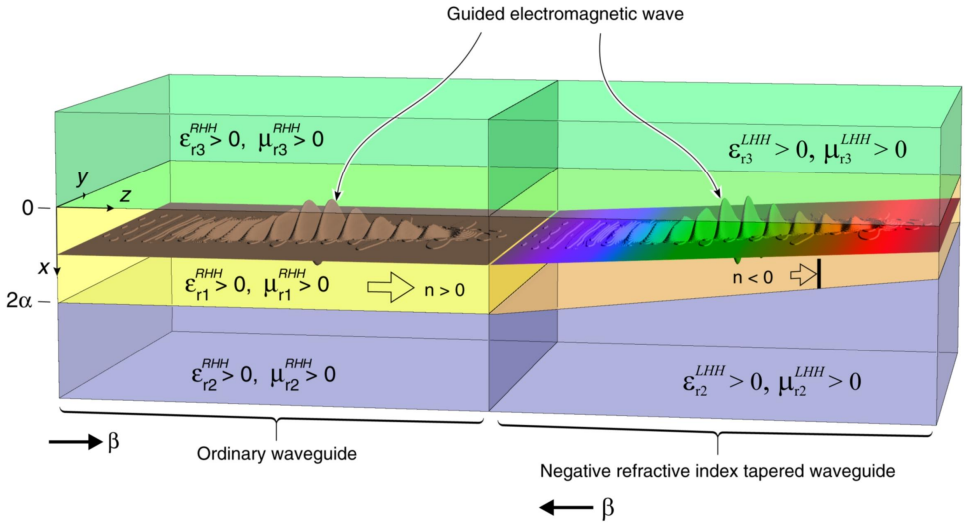

Fig. 1. Schematic illustration of an oscillatory wave guided along an ordinary dielectric waveguide and coupled to an adiabatically tapered left-handed heterostructure. Each frequency component ('color') of the wave stops at correspondingly different point inside the tapered negative-index waveguide, forming a 'trapped rainbow'.

From Eq. (4), it follows that by requiring at each segment of the tapered waveguide:

$$F = 2\sigma_\varepsilon U \left[\frac{\omega\varepsilon_0 |\varepsilon_{r1}| P_{\text{tot}}^{\text{con}}}{\alpha\beta (W_3^2 + \sigma_\varepsilon^2 U^2) \Theta} \right]^{1/2}, \tag{5}$$

with Θ being equal to the summation inside the parenthesis of Eq. (3), we ensure that the guided electromagnetic field carries a constant (conserved) total power flow, equal to $P_{\text{tot}}^{\text{con}}$, throughout the LHH. Note that the fields are normalised with respect to $P_{\text{tot}}^{\text{con}}$, *not* $P_{\text{tot}}^{+z} = 1/2 \int_{-\infty}^{\infty} \text{Re}(\mathbf{E} \times \mathbf{H}^*)_z \, dx$, since the latter one does not remain constant along the LHH, as in regular dielectric guides but, instead, it continuously decreases until it becomes zero at the 'critical' guide thickness. Normalising the fields with P_{tot}^{+z} instead of $P_{\text{tot}}^{\text{con}}$, would have caused their unphysical divergence at the point where they are stopped.

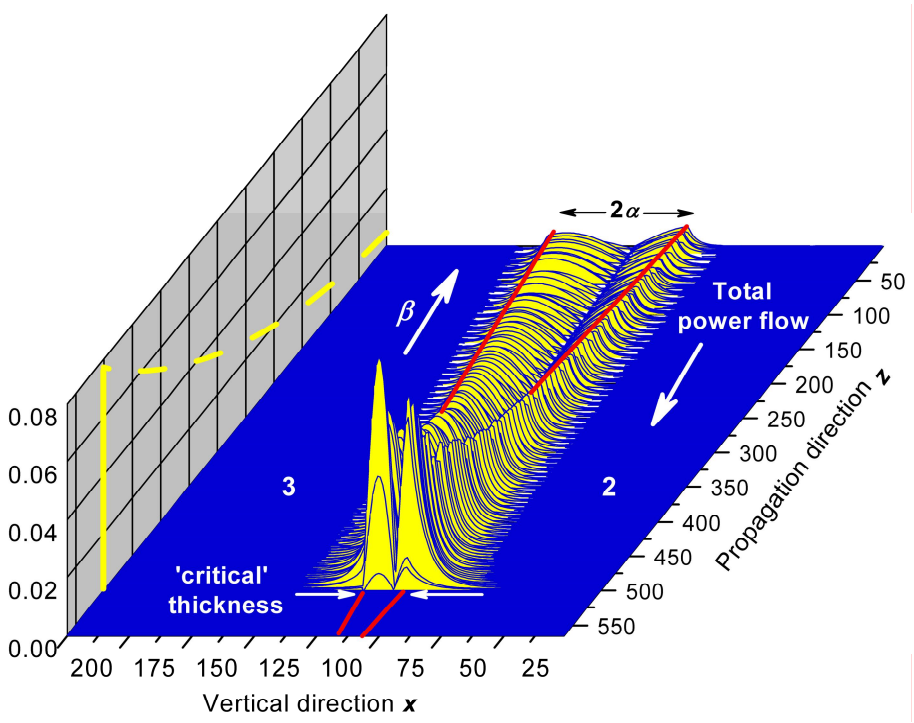

Fig. 2. Monochromatic wave propagation along an adiabatically tapered waveguide with a negative refractive index core. Shown is the H_y-field component of the propagating, second-order, *p*-polarised waveguide mode. The two solid red lines indicate the thickness of the core layer, while the dashed yellow line at the left vertical plane of the figure designates the progressive increase in the amplitude of the propagating magnetic component.

Figure 2 illustrates an exemplary result of such calculations. Shown is a snapshot from the propagation and complete halting of a monochromatic wave of frequency $f = 1$ THz, carrying a total, conserved, time-averaged power-flow $P_{\text{tot}}^{\text{con}} = 82.6\ \mu\text{W/m}^2/\text{sec}$. The core layer has refractive index $n_1 = -5$, while the refractive indices of the two dielectric cladding layers are $n_2 = 1.6$ and $n_3 = 1.5$. The wave propagates smoothly down the waveguide, and at the 'critical' thickness of $ak_0 = 0.55$ it altogether stops ($v_g = 0$). Moreover, one clearly observes that while approaching the 'critical' thickness, the amplitude of the sole magnetic field component progressively increases and the wave becomes spatially compressed, as anticipated from the "slow-light" theory [14]. We also note that, while propagating, the wave is in the "negative phase velocity" mode, i.e. the directions of the time-averaged power flow P_{tot}^{+z} and the longitudinal propagation constant β are antiparallel. It is interesting to note that, owing to the anomalous frequency dispersion associated with the metamaterial heterostructure, larger wave frequencies (i.e. *smaller* free-space wavelengths) are stopped at *larger* core thicknesses, as illustrated in Fig. 1.

2.2 Ray analysis of wave propagation in NRI waveguide

In the previous section we showed that the guided electromagnetic wave completely stops, without being back-reflected, upon reaching the 'critical' guide thickness, since at that point its total time-averaged power (flow) becomes zero and so does its group velocity. In fact, it swiftly turns out from a pertinent time-domain analysis that the wave takes infinitely long time before it arrives at *exactly* the 'critical' point, i.e. the associated time diverges logarithmically with the distance from that point. It is also important to note that the vanishing group velocity of the wave does not necessarily prove that the wave will stop. For instance, Fig. 3 illustrates a familiar situation from classical mechanics,

wherein a tennis ball hitting a vertical wall assumes zero velocity before being reflected back; this is, obviously, because the total energy (kinetic + dynamic) of the ball is not zero at the point where **u** = 0 and, as a result, the stored dynamic energy is converted back to kinetic energy and the ball starts moving backwards. In our case, the wave stops because at the 'hitting' point its *total*, time-averaged, power vanishes and the time the wave needs to reach that point diverges.

A much clearer and more intuitive picture of how exactly the wave is stopped can be obtained by tracing the trajectory of the associated light ray (of the monochromatic wave) along its zigzag path. To this end, let us assume that a ray of *p*-polarised light impinges upon the 1-3 media interface with angle θ. Following a course of analysis similar to that followed for dielectric waveguides, one may show that the associated Goos-Hänchen phase shift will be [22, 25]:

$$\delta_{p13} = -2\tan^{-1}\left(\frac{W_3}{\sigma_\varepsilon U}\right). \tag{6}$$

For the sake of convenience in the subsequent algebraic manipulations, let us rewrite Eq. (6) in the following form:

$$\delta_{p13} = -2\tan^{-1}(f(\theta)) = -2\tan^{-1}\left[\frac{(\sin^2\theta - \sigma_\varepsilon\sigma_\mu)^{1/2}}{\sigma_\varepsilon\cos\theta}\right], \tag{7}$$

with $\sigma_\mu = \mu_{r3}/|\mu_{r1}|$, from whence we obtain:

$$\frac{df(\theta)}{d\theta} = \frac{(1-\sigma_\varepsilon\sigma_\mu)\sin\theta}{\sigma_\varepsilon\cos^2\theta(\sin^2\theta - \sigma_\varepsilon\sigma_\mu)^{1/2}}, \tag{8}$$

$$\frac{d}{d\theta}\{\tan^{-1}[f(\theta)]\} = \frac{\sigma_\varepsilon(1-\sigma_\varepsilon\sigma_\mu)\sin\theta}{(\sin^2\theta - \sigma_\varepsilon\sigma_\mu)^{1/2}[(\sigma_\varepsilon^2 - 1)\cos^2\theta + (1-\sigma_\varepsilon\sigma_\mu)]}. \tag{9}$$

The inverted 'penetration' distance, x_{p13}, can now be calculated by means of the following relationship:

$$x_{p13} = \frac{1}{k_0 |n_1| \sin\theta}\frac{d}{d\theta}\{\tan^{-1}[f(\theta)]\}, \tag{10}$$

and we successively have:

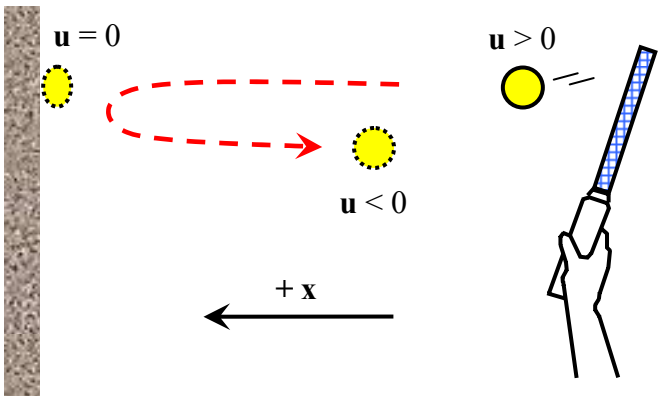

Fig. 3. Schematic illustration of a tennis ball hitting a vertical wall and being reflected backwards.

$$x_{p13} = \frac{\sigma_\varepsilon}{k_0 (n_1^2 \sin^2\theta - n_3^2)^{1/2}} \frac{1 - \sigma_\varepsilon \sigma_\mu}{(\sigma_\varepsilon^2 - 1)\cos^2\theta + (1 - \sigma_\varepsilon \sigma_\mu)} = \tag{11a}$$

$$= \frac{\sigma_\varepsilon}{\gamma_3} \frac{n_1^2 - n_3^2}{\sigma_\varepsilon^2 \dfrac{\kappa^2}{k_0^2} - \dfrac{\kappa^2}{k_0^2} + n_1^2 - n_3^2} = \tag{11b}$$

$$= \frac{\sigma_\varepsilon}{\gamma_3} \frac{n_1^2 - n_3^2}{\sigma_\varepsilon^2 \dfrac{\kappa^2 (n_1^2 - n_3^2)}{\gamma_3^2 + \kappa^2} - \dfrac{\kappa^2 (n_1^2 - n_3^2)}{\gamma_3^2 + \kappa^2} + n_1^2 - n_3^2} = \tag{11c}$$

$$= \frac{\sigma_\varepsilon}{\gamma_3} \frac{\gamma_3^2 + \kappa^2}{\gamma_3^2 + \sigma_\varepsilon^2 \kappa^2}, \tag{11d}$$

where we used the identity $k_0^2 = (\gamma_3^2 + \kappa^2)/(n_1^2 - n_2^2)$. From Eq. (11d), it directly follows that:

$$x_{p13} = \frac{\alpha \sigma_\varepsilon}{W_3} \frac{V_3^2}{W_3^2 + \sigma_\varepsilon^2 U^2}, \tag{12}$$

which is the relation for the distance between the rays' cross points and the 1-3 media interface. In a similar vein, one can prove that:

$$x_{p12} = \frac{\alpha \rho_\varepsilon}{W_2} \frac{V_2^2}{W_2^2 + \rho_\varepsilon^2 U^2}. \tag{13}$$

Let us, now, derive an expression associating the time-averaged power flow propagating in the increasing +z direction with the effective thickness of the left-handed heterostructure, similar to the relations that hold for conventional dielectric heterostructures [22, 26]. We recall that the solution ansatz to the wave equation for the p-polarised oscillatory waveguide modes supported by the LHH has the following form:

$$H_y = \begin{cases} Fe^{\gamma_3 x}, & x \le 0 \\ G\cos(\kappa x) + K\sin(\kappa x), & 0 \le x \le 2\alpha \\ Le^{-(x-2\alpha)\gamma_2}, & x \ge 2\alpha \end{cases}, \tag{14}$$

where $G = F$, $K = -\dfrac{\gamma_3}{\sigma_\varepsilon \kappa} F$, $L = [\cos(2\alpha\kappa) - \dfrac{\gamma_3}{\sigma_\varepsilon \kappa}\sin(2\alpha\kappa)]F$, and $E_z = \dfrac{\mathrm{i}}{\omega\varepsilon}\dfrac{\partial H_y}{\partial x}$, $E_x = \dfrac{\beta}{\omega\varepsilon} H_y$. From Eq. (14) we deduce that the maximum value for the H_y field component is $H_y^{\max} = F\dfrac{(W_3^2 + \sigma_\varepsilon^2 U^2)^{1/2}}{\sigma_\varepsilon U}$, and occurs within the middle layer-1 at point $x^{\max} = \dfrac{\alpha}{U}\tan^{-1}\left(-\dfrac{W_3}{\sigma_\varepsilon U}\right)$. After some algebraic manipulations, we can analytically calculate the total time-averaged power flow in the increasing +z direction, P_{tot}^{+z}, as [23, 24, 28]:

$$P_{\text{tot}}^{+z}\Big|_{LHH} = \left(\frac{F^2}{4\omega\varepsilon_0}\right)\frac{W_3^2+\sigma_\varepsilon^2U^2}{\sigma_\varepsilon^2U^2}\frac{\alpha\beta}{|\varepsilon_{r1}|}\left(\underbrace{\frac{\rho_\varepsilon}{W_2}\frac{V_2^2}{W_2^2+\rho_\varepsilon^2U^2}}_{x_{p12}/\alpha}+\underbrace{\frac{\sigma_\varepsilon}{W_3}\frac{V_3^2}{W_3^2+\sigma_\varepsilon^2U^2}}_{x_{p13}/\alpha}-2\right), \tag{15}$$

from whence we immediately obtain:

$$P_{\text{tot}}^{+z} = \frac{1}{4}E_x^{\max}H_y^{\max}t_{eff}, \tag{16}$$

where $t_{eff} = 2\alpha - x_{p12} - x_{p13}$ is effective thickness of the left-handed heterostructure. Note that, owing to the negativeness of the permittivity ε_1 in the core of the LHH, the term $E_x^{\max}H_y^{\max}$ in the right-hand side of Eq. (16) is always negative;

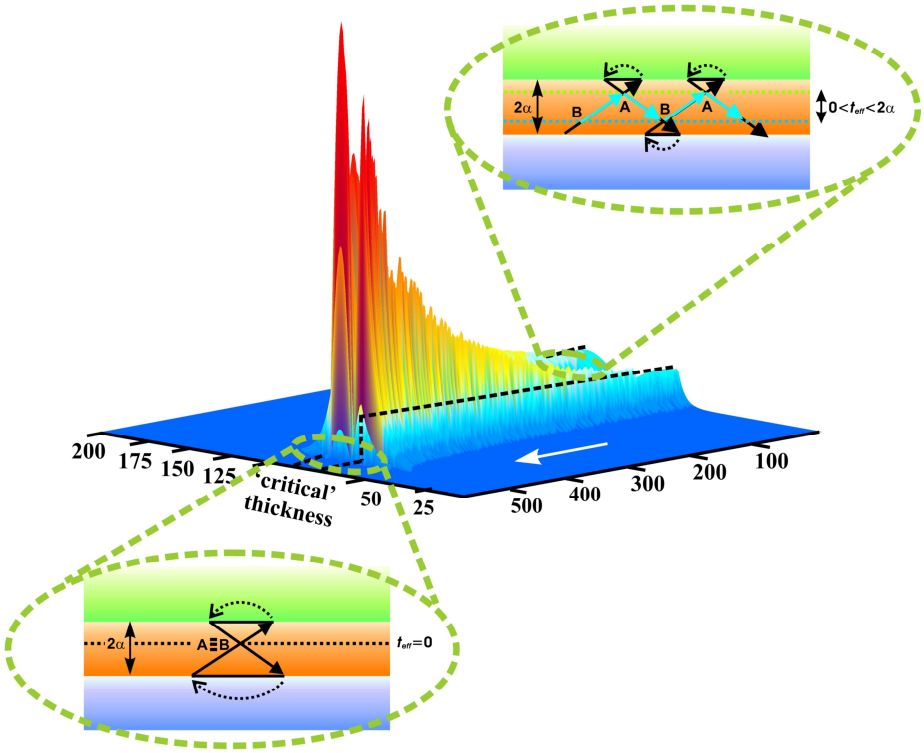

Fig. 4. Association of wave propagation inside the adiabatically tapered NRI waveguide with the corresponding zigzag ray analysis for different guide widths. The optogeometric parameters are those of Fig. 2.

hence, P_{tot}^{+z} and t_{eff} are oppositely signed. It is should be herein noted that a negative P_{tot}^{+z} corresponds to a negative phase velocity mode (P_{tot}^{+z} antiparallel to the mode longitudinal propagation constant β) and a positive P_{tot}^{+z} to a positive where $t_{eff} = 2\alpha - x_{p12} - x_{p13}$ is effective thickness of the left-handed heterostructure. Note that, owing to the negativeness of the permittivity ε_1 in the core of the LHH, the term $E_x^{\max}H_y^{\max}$ in the right-hand side of Eq. (16) is always negative;
hence, P_{tot}^{+z} and t_{eff} are oppositely signed. It is should be herein noted that a negative P_{tot}^{+z} corresponds to a negative

phase velocity mode (P_{tot}^{+z} antiparallel to the mode longitudinal propagation constant β) and a positive P_{tot}^{+z} to a positive phase velocity mode (P_{tot}^{+z} and β are parallel). Eq. (16) reveals that at the "critical" physical core thickness all three quantities, i.e. group velocity, time-averaged power-flow and guide *effective* thickness, simultaneously vanish.

By means of Eqs. (15) and (16) we may, hence, deduce that, in stark contrast to conventional dielectric waveguides, in NRI heterostructures the effective thickness t_{eff} is always smaller that the core physical thickness 2α, and can become zero or even negative. An example of zero effective NRI waveguide thickness is illustrated in the top left inset of Fig. 5. For the set of optogeometric parameters corresponding to that inset, the two Goos-Hänchen phase shifts experienced by the ray upon hitting the two media interfaces are such that $x_{p12} + x_{p13} = 2\alpha$ exactly (see Fig. 4, bottom left inset). As a result, the light ray becomes permanently trapped, forming a double light-ray cone, which (in view of its characteristic hourglass form) we call 'optical clepsydra'.

2.3 In-coupling from a conventional dielectric waveguide to a NRI heterostructure

Here we show that efficient in-coupling from a conventional dielectric waveguide to the previously described NRI heterostructure can, indeed, be achieved. To demonstrate that, we start by calculating the characteristic impedances of both structures. To this endeavour, we use the "power-voltage" definition of the characteristic impedance in waveguide structures [27, 28], beginning by calculating a 'voltage' V_0 across each waveguide by means of the following relation:

$$V_0 = \int_{-\infty}^{\infty} E_x dx = \frac{\beta}{\omega} \int_{-\infty}^{\infty} \frac{H_y}{\varepsilon} dx. \tag{17}$$

We may then obtain the following expressions for the voltages V_i (i = 1, 2, 3) crosswise each i-layer of the NRI heterostructure:

$$V_1^{LHH} = -\left(\frac{F}{\omega\varepsilon_0}\right)\frac{\alpha\beta}{|\varepsilon_{r1}|}\frac{\sqrt{W_3^2 + \sigma_\varepsilon^2 U^2}}{\sigma_\varepsilon U^2}\left(\pm\frac{W_2}{\sqrt{W_2^2 + \rho_\varepsilon^2 U^2}} - \frac{W_3}{\sqrt{W_3^2 + \sigma_\varepsilon^2 U^2}}\right), \tag{18}$$

$$V_2^{LHH} = \mp\left(\frac{F}{\omega\varepsilon_0}\right)\frac{\alpha\beta}{|\varepsilon_{r1}|}\frac{1}{\sigma_\varepsilon W_2}\frac{\sqrt{W_3^2 + \sigma_\varepsilon^2 U^2}}{\sqrt{W_2^2 + \rho_\varepsilon^2 U^2}}, \tag{19}$$

$$V_3^{LHH} = \left(\frac{F}{\omega\varepsilon_0}\right)\frac{\alpha\beta}{|\varepsilon_{r1}|}\frac{1}{\sigma_\varepsilon W_3}, \tag{20}$$

from whence we find:

$$V_0^{LHH} = \sum_{i=1}^{3} V_i^{LHH} = \left(\frac{F}{\omega\varepsilon_0}\right)\frac{\alpha\beta}{|\varepsilon_{r1}|}\frac{\sqrt{W_3^2 + \sigma_\varepsilon^2 U^2}}{\sigma_\varepsilon U^2}\left(\mp\frac{V_2^2}{W_2\sqrt{W_2^2 + \rho_\varepsilon^2 U^2}} + \frac{V_3^2}{W_3\sqrt{W_3^2 + \sigma_\varepsilon^2 U^2}}\right), \tag{21}$$

where the "+" (plus) sign is used for $U \in [(m-1/4)\pi,\ (m+1/4)\pi]$ and the "–" (minus) sign for $U \in [(m+1/4)\pi,\ (m+3/4)\pi]$, with $m \in \mathbf{N}$, U > 0.

In a similar vein, using Eq. (14) and the parameter definitions that follow it, we obtain the following expressions for the V_i (i = 1, 2, 3) voltages of the dielectric waveguide:

$$V_1^{RHH} = \left(\frac{F}{\omega\varepsilon_0}\right)\frac{\alpha\beta}{\varepsilon_{r1}}\frac{\sqrt{W_3^2+\sigma_\varepsilon^2U^2}}{\sigma_\varepsilon U^2}\left(\pm\frac{W_2}{\sqrt{W_2^2+\rho_\varepsilon^2U^2}}+\frac{W_3}{\sqrt{W_3^2+\sigma_\varepsilon^2U^2}}\right), \tag{22}$$

$$V_2^{RHH} = \pm\left(\frac{F}{\omega\varepsilon_0}\right)\frac{\alpha\beta}{\varepsilon_{r1}}\frac{1}{\sigma_\varepsilon W_2}\frac{\sqrt{W_3^2+\sigma_\varepsilon^2U^2}}{\sqrt{W_2^2+\rho_\varepsilon^2U^2}}, \tag{23}$$

$$V_3^{RHH} = \left(\frac{F}{\omega\varepsilon_0}\right)\frac{\alpha\beta}{\varepsilon_{r1}}\frac{1}{\sigma_\varepsilon W_3}, \tag{24}$$

from whence we find:

$$V_0^{RHH} = \sum_{i=1}^{3} V_i^{RHH} = \left(\frac{F}{\omega\varepsilon_0}\right)\frac{\alpha\beta}{\varepsilon_{r1}}\frac{\sqrt{W_3^2+\sigma_\varepsilon^2U^2}}{\sigma_\varepsilon U^2}\left(\pm\frac{V_2^2}{W_2\sqrt{W_2^2+\rho_\varepsilon^2U^2}}+\frac{V_3^2}{W_3\sqrt{W_3^2+\sigma_\varepsilon^2U^2}}\right), \tag{25}$$

where the use of the "+" (plus) and "–" (minus) signs follows the same rule as in the case of the LHH. Moreover, one can show that the time-averaged power flow propagating in the increasing $+z$ direction inside the RHH is given by [26]:

$$P_{\text{tot}}^{+z}\Big|_{RHH} = \left(\frac{F^2}{4\omega\varepsilon_0}\right)\frac{W_3^2+\sigma_\varepsilon^2U^2}{\sigma_\varepsilon^2U^2}\frac{\alpha\beta}{\varepsilon_{r1}}\left(2+\frac{\rho_\varepsilon}{W_2}\frac{V_2^2}{W_2^2+\rho_\varepsilon^2U^2}+\frac{\sigma_\varepsilon}{W_3}\frac{V_3^2}{W_3^2+\sigma_\varepsilon^2U^2}\right). \tag{26}$$

By means of the power-voltage definition of the waveguide characteristic impedance [27]:

$$Z_0^{PV} = \frac{|V_0|^2}{2P_{\text{tot}}^{+z}}, \tag{27}$$

using Eqs. (15) and (21) for the NRI heterostructure, or Eqs. (25) and (26) for the dielectric waveguide, one can now directly calculate the impedance for each waveguide. We note from Eq. (27) that the characteristic impedance of the left-handed heterostructure diverges at the 'critical' guide thickness, as anticipated, since in this case the heterostructure is in the 'stopped light regime' and, hence, the corresponding light signal can not penetrate it and propagate inside.

Using the above relations, one finds that for the NRI heterostructure analysed before (Fig. 4) and for a conventional optical waveguide with $n_{core} = 1.25$, $n_{cladding2} = 1.2$ and $n_{cladding3} = 1.1$, we can achieve complete impedance matching for a reduced guide thickness, ak_0, equal to approximately 12.77. In addition to the impedance and thickness matching at that point, it also promptly turns out that the two structures have very similar magnetic field distributions (mode matching). As a result, a wave launched from the dielectric waveguide to the left-handed heterostructure will experience minimal reflection, mainly owing to minute mode-mismatch, which in practice can be further adjusted and optimised at will.

3. CONCLUSIONS

In summary, we have shown how guided electromagnetic energy can efficiently be brought to a complete standstill whilst travelling inside axially varying NRI waveguiding heterostructures. By nature, the scheme invokes solid-state materials and, as such, is not subject to low-temperature or atomic coherence limitations. Moreover, it inherently allows for high in-coupling efficiencies and broadband function, since the deceleration of light does not rely on refractive index resonances. This method for trapping photons opens the way to a multitude of hybrid, optoelectronic devices to be used

in ‘quantum information’ processing, communication networks and signal processors, and conceivably heralds a new realm of combined metamaterials and slow light research.

ACKNOWLEDGEMENTS

This work was supported by the Engineering and Physical Sciences Research Council (UK). We also wish to acknowledge useful discussions with Allan D. Boardman and John Pendry.

REFERENCES

1. T. J. Yen, W. J. Padilla, N. Fang, D. C. Vier, D. R. Smith, J. B. Pendry, D. N. Basov, and X. Zhang, *Science* **303**, 1494 (2004).
2. A. N. Grigorenko, A. K. Geim, H. F. Gleeson, Y. Zhang, A. A. Firsov, I. Y. Khrushchev, and J. Petrovic, *Nature* (London) **438**, 17 (2005)
3. V. M. Shalaev, *Nature Photonics* **1**, 41 (2007).
4. W. E. Kock, *Bell System Technical J*. **34**, 828 (1946).
5. R. E. Collin, *Field Theory of Guided Waves* (IEEE Press, 2nd ed., 1991), ch. 12.
6. W. Rotman, *IRE Trans. Antennas Propagat*. **10**, 82 (1962).
7. V. G. Veselago, *Sov. Phys. Usp*. **10**, 509 (1968).
8. V. G. Veselago, in *Proceedings of the First Taormina Research Conference on the Structure of Mater, Pergamon, 1972*, edited by E. Burstein and F. De Martini (Pergamon Press, New York, 1974), p. 5.
9. J. B. Pendry, *Phys. Rev. Lett*. **85**, 3966 (2000).
10. R. A. Shelby, D. R. Smith, and S. Shultz, *Science* **292**, 77 (2001).
11. A. N. Lagarkov and V. N. Kissel, *Phys. Rev. Lett*. **92**, 077401 (2004).
12. G. V. Eleftheriades and K. G. Balmain, *Negative Refraction Metamaterials: Fundamental Principles and Applications* (Wiley-IEEE, New Jersey, 2005).
13. A. Alù and N. Engheta, *Phys. Rev. B* **75**, 024304 (2007).
14. P. W. Milonni, *Fast light, Slow Light and Left-Handed Light* Chs. 5 & 6 (Institute of Physics, Bristol, 2005).
15. C. Liu, Z. Dutton, C. H. Behroozi, and L. V. Hau *Nature* (London) **409**, 490 (2001).
16. E. Gehrig, M. van der Poel, J. Mørk, and O. Hess, *IEEE J. Quantum Electron.* **42**, 1047 (2006).
17. Y. A. Vlasov, M. O'Boyle, H. F. Hamann, and S. J. McNab, *Nature* (London) **438**, 65 (2005).
18. M. S. Bigelow, N. N. Lepeshkin, and R. W. Boyd, *Science* **301**, 200 (2003).
19. Y. Okawachi, *et al*., *Phys. Rev. Lett*. **94**, 153902 (2005).
20. M. I. Stockman, *Phys. Rev. Lett*. **93**, 137404 (2004).
21. A. Karalis, E. Lidorikis, M. Ibanescu, J. D. Joannopoulos, and M. Soljačić, *Phys. Rev. Lett*. **95**, 063901 (2005).
22. A. Snyder and J. D. Love, *Optical Waveguide Theory* Chs. 5 & 19 (Chapman and Hall, New York, 1983).
23. K. L. Tsakmakidis, A. Klaedtke, C. Jamois, D. P. Aryal, and O. Hess, *Appl. Phys. Lett*. **89**, 201103 (2006).
24. K. L. Tsakmakidis, C. Hermann, A. Klaedtke, C. Jamois, and O. Hess, *Phys. Rev. B* **73**, 085104 (2006).
25. P. R. Berman, *Phys. Rev. E* **66**, 067603 (2002).
26. T. Tamir (Ed.), *Integrated Optics* Ch. 2 (Springer-Verlag, New York, 1979).
27. J. Helszajn, *Ridge Waveguides and Passive Microwave Components* (IEE Press, London, 2000).
28. K. L. Tsakmakidis, A. D. Boardman, and O. Hess, *Nature* (London) **450**, 397 (2007).